Distinct Cellular Locations of Carbonic Anhydrases Mediate Carbon Dioxide Control of Stomatal Movements[1][OPEN]

Honghong Hu*, Wouter-Jan Rappel, Rossana Occhipinti, Amber Ries, Maik Böhmer[2], Lei You, Chuanlei Xiao, Cawas B. Engineer, Walter F. Boron, and Julian I. Schroeder*

College of Life Science and Technology, Huazhong Agricultural University, Wuhan 430070, China (H.H., L.Y., C.X.); Division of Biological Sciences, Cell and Developmental Biology Section (H.H., A.R., M.B., C.B.E., J.I.S.) and Physics Department (W.-J.R.), University of California, San Diego, La Jolla, California 92093–0116; and Department of Physiology and Biophysics (R.O., W.F.B.) and Department of Medicine (W.F.B.), Case Western Reserve University School of Medicine, Cleveland, Ohio 44106

ORCID IDs: 0000-0003-0538-6646 (H.H.); 0000-0001-6675-273X (M.B.).

Elevated carbon dioxide (CO_2) in leaves closes stomatal apertures. Research has shown key functions of the β-carbonic anhydrases (βCA1 and βCA4) in rapid CO_2-induced stomatal movements by catalytic transmission of the CO_2 signal in guard cells. However, the underlying mechanisms remain unclear, because initial studies indicate that these Arabidopsis (*Arabidopsis thaliana*) βCAs are targeted to distinct intracellular compartments upon expression in tobacco (*Nicotiana benthamiana*) cells. Which cellular location of these enzymes plays a key role in native guard cells in CO_2-regulated stomatal movements remains unknown. Here, we express fluorescently tagged CAs in guard cells of *ca1ca4* double-mutant plants and show that the specific locations of βCA4 at the plasma membrane and βCA1 in native guard cell chloroplasts each can mediate rapid CO_2 control of stomatal movements. Localization and complementation analyses using a mammalian αCAII-yellow fluorescent protein in guard cells further show that cytoplasmic localization is also sufficient to restore CO_2 regulation of stomatal conductance. Mathematical modeling of cellular CO_2 catalysis suggests that the dynamics of the intracellular HCO_3^- concentration change in guard cells can be driven by plasma membrane and cytoplasmic localizations of CAs but not as clearly by chloroplast targeting. Moreover, modeling supports the notion that the intracellular HCO_3^- concentration dynamics in guard cells are a key mechanism in mediating CO_2-regulated stomatal movements but that an additional chloroplast role of CAs exists that has yet to be identified.

Diverse roles of carbonic anhydrases (CAs) in a broad range of biochemical processes have been investigated such as carboxylation or decarboxylation reactions, including photosynthesis and respiration. CAs are some of the most rapid enzymes known that facilitate the catalysis of CO_2 and water to bicarbonate and protons. CA proteins can be grouped into several major distinct classes (α, β, and γ; Hewett-Emmett and Tashian, 1996; Tripp et al., 2001) and also, δ- and ε-classes (Lane and Morel, 2000; So et al., 2004). To date, all CAs identified in animal systems belong to α-class, whereas in plants and algae, known CAs are more diverse, belonging to the α-, β-, γ-, and δ-classes.

In algae, a key function of CAs is in the CO_2-concentrating mechanism, which concentrates inorganic carbon for efficient photosynthetic activity (Badger and Price, 2003; Spalding, 2008; Moroney et al., 2011; Wang et al., 2011; Ludwig, 2012). In the microalga *Chlamydomonas reinhardtii*, two periplasmic αCAs function in supplying inorganic carbon for photosynthesis (Fukuzawa et al., 1990), and mitochondria-localized βCAs are involved in converting CO_2 produced in mitochondria into HCO_3^- (Raven, 2001; Giordano et al., 2003). In C4 plants, CAs provide HCO_3^- to phosphoenolpyruate carboxylase to produce the C4 acid oxaloacetic acid. The cytosolic βCA in *Flaveria bidentis* was identified to function in, but is not rate limiting for, C4 photosynthesis as found in antisense suppression analyses (von Caemmerer et al., 2004). It has been suggested that CA activity in C4 plants is near rate limiting for photosynthesis (Hatch and Burnell, 1990; Cousins et al., 2008). A recent study in maize (*Zea mays*) showed that CAs are not limiting for C4 photosynthesis, at least at current ambient CO_2 conditions, but become limiting at low CO_2 concentrations in leaves (partial pressure of CO_2 inside leaf [C_i]; Studer et al., 2014). Photosynthetic rates in maize *ca1ca2* double-mutant plants were not reduced under current and elevated CO_2 partial pressures but were impaired at low partial pressures (Studer et al., 2014). In C3 plants, the roles of CAs in limiting photosynthesis are less clear, but γCAs do have biological roles in mitochondrial physiology (Perales et al., 2005) and function in male sterility (Villarreal et al., 2009).

In addition to the roles of CAs in biochemical processes, recent research has shown that CAs function in animal CO_2 signaling pathways. An αCA has been identified in mice as a CO_2 perception mechanism controlling the olfactory response of guanylyl cyclase D neurons (GC-D+) to CO_2 that triggers an avoidance behavior (Hu et al., 2007). An inhibitor of CAs reduces the ability of rodents to detect CO_2, providing pharmacological evidence that CAs function as olfactory CO_2 receptors (Ferris et al., 2007; Hu

et al., 2007). It was found that CO_2-induced action potentials occur in nerves that connect to taste receptors (sour sensing) cells in the mouse tongue (Chandrashekar et al., 2009). When taste receptor cells in which the carbonic anhydrase4 (Car4) is expressed at the surface were ablated in the mouse tongue, the response to CO_2 disappeared, indicating that CA is an essential component of the CO_2 response linked with sour taste (Chandrashekar et al., 2009).

In plants, CO_2 signaling mechanisms control stomatal movements. Stomata in the epidermis of aerial tissues enable CO_2 influx for photosynthesis (Cardon et al., 1994; DeLucia et al., 1999; Medlyn et al., 2001; Hetherington and Woodward, 2003). Guard cells that form stomatal pores have mechanisms to respond to an increase in the CO_2 concentration in leaves (C_i), resulting in closing of stomatal pores. However, how elevated CO_2 is transduced in guard cells remains less understood. Two βCAs, CA1 and CA4, were identified that function in the CO_2 response (Hu et al., 2010). Arabidopsis (*Arabidopsis thaliana*) plants lacking these two enzymes displayed slowed stomatal responses to CO_2 changes (Hu et al., 2010), and these impaired CO_2 responses can be restored by expression of either *βCA1*, *βCA4*, or an unrelated human *αCAII* in guard cells using a strong guard cell promoter (Hu et al., 2010). These findings support the hypotheses that the enzymatic activities of βCA1 and βCA4 mediate the stomatal CO_2 response and that these βCAs do not function as noncatalytic CO_2 receptors. Additional electrophysiological analyses showed that intracellular HCO_3^- ions in guard cells lead to enhanced activation of guard cell anion channels and together with the above analyses, suggest that this stomatal CO_2 response mediated by βCA1/βCA4 can be perceived directly by guard cells (Xue et al., 2011).

Additional findings identified GROWTH CONTROL BY ABSCISIC ACID2 (GCA2), OPEN STOMATA1 (OST1), and SLOW ANION CHANNEL-ASSOCIATED1 (SLAC1) as positive regulators (Young et al., 2006; Negi et al., 2008; Vahisalu et al., 2008; Xue et al., 2011) and the HIGH LEAF TEMPERATURE1 (HT1) kinase and a malate uptake transporter ATP-BINDING CASSETTE B14 (AtABCB14) as negative regulators (Hashimoto et al., 2006; Lee et al., 2008) in the high CO_2-induced stomatal closing signaling pathway. A current molecular genetic and physiological model of this pathway was proposed: elevated CO_2 accelerates the conversion by βCA1 and βCA4 into bicarbonate; elevated bicarbonate together with CO_2 act as an intracellular messenger to activate S-type anion channels through OST1, thus triggering closure of stomata (Xue et al., 2011). Recently, the RESISTANT TO HIGH CARBON DIOXIDE1 (RHC1) MULTIDRUG AND TOXIC COMPOUND EXTRUSION (MATE) transmembrane protein was reported to function as an HCO_3^- sensing protein, interact with HT1, and release OST1 to phosphorylate SLAC1 channels (Tian et al., 2015). Beyond the function of βCA1 and βCA4 in CO_2 control of stomatal movements, βCA1 and βCA4 were also identified as functioning in CO_2 regulation of stomatal development together with the secreted EPIDERMAL PATTERNING FACTOR2 (EPF2) signaling peptide and a secreted protease CARBON DIOXIDE RESPONSE SECRETED PROTEASE (CRSP) in a distinct OST1-independent pathway (Engineer et al., 2014). Leaf epidermes of *ca1ca4* plants exhibit an enhancement in stomatal density and index upon CO_2 elevation compared with low CO_2-grown plants, in contrast to wild-type plants.

Previous research has suggested that the enzymatic activity of βCA1 and βCA4 functions in CO_2 control of stomatal movements (Hu et al., 2010; Xue et al., 2011). However, βCA1 and βCA4 were found at different cellular locations when expressed in tobacco (*Nicotiana benthamiana*) cells (Fabre et al., 2007; Hu et al., 2010), and which cellular location of these enzymes plays a key role in CO_2-regulated stomatal movements and thus, the underlying mechanisms has remained unclear. Previous research did not use fluorescent protein fusion constructs to localize individual CAs in their native guard cells in complementation lines; therefore, the required cellular localizations of CAs for mutant complementation have remained unknown, and the relevance of these cellular locations remains unknown (Hu et al., 2010). It seems likely that overexpression in guard cells could have resulted in overlapping cellular localizations,

[1] This work was supported by the National Science Foundation (grant no. MCB1414339 to J.I.S. and W.J.R.). Chloroplast targeting analyses of CAs were funded by the Division of Chemical, Geo, and Biosciences, Office of Basic Energy Sciences, U.S. Department of Energy (grant no. DE–FG02–03ER15449 to J.I.S.) and the National Institutes of Health (grant no. GM060396 to J.I.S.). Research at Huazhong Agricultural University was funded by the China National Natural Science Foundation (grant no. 31271515), the Program for New Century Excellent Talents in University (NCET–12–0861), and the Fundamental Research Funds for the Central Universities (projects 2662013PY019 and 2662013JQ002 to H.H.). Research of R.O. and W.F.B. was funded by the Office of Naval Research (grant no. N00014–11–1–0889, N00014–14–1–0716), National Institutes of Health (grant no. U01–GM111251), and the Meyer/Scarpa Chair to W.F.B. C.E. was supported in part by the San Diego Center for Systems Biology (Systems Biology seed grant no. GM085764).

[2] Present address: Institute for Biology and Biotechnology of Plants, Westfälische Wilhelms-University, Schlossplatz 7, 48149 Muenster, Germany.

* Address correspondence to huhh@mail.hzau.edu.cn and jischroeder@ucsd.edu.

The author responsible for distribution of materials integral to the findings presented in this article in accordance with the policy described in the Instructions for Authors (www.plantphysiol.org) is: Julian I. Schroeder (jischroeder@ucsd.edu).

H.H. performed most of the experiments at the University of California, San Diego, analyzed the data, and cowrote the article; W.-J.R., R.O., and W.F.B. conducted the mathematical modeling of cellular CO_2 catalysis and revised the article; M.B. performed the tandem mass spectrometry analysis of *βCA1* in tobacco (*Nicotiana benthamiana*); C.X. analyzed the subcellular localization of different deletions of CA1 in tobacco; A.R. and L.Y. generated transgenic plants and helped with gas exchange analyses; C.B.E. performed some of the gas exchange analyses and contributed to the article writing; H.H. and J.I.S. conceived the project, cowrote the article, and revised the article.

[OPEN] Articles can be viewed without a subscription.
www.plantphysiol.org/cgi/doi/10.1104/pp.15.00646

and this might explain the complementation of stomatal conductance phenotypes by either CA alone.

In this study, we used yellow fluorescent protein (YFP) or GFP protein fusions to cellularly localize the individual CAs, βCA1 or βCA4, while in parallel, determining their effects on CO_2-regulated stomatal responses. We report here that the βCA4 at the plasma membrane and βCA1 in chloroplasts each function in CO_2 control of stomatal conductance changes. Together with combined targeting and complementation analyses with a nucleo/cytoplasmically localized mammalian *αCAII* expressed in guard cells and mathematical modeling of CO_2 fluxes and catalysis by CAs in guard cells, the presented data suggest that the intracellular rate of bicarbonate concentration changes in guard cells is a key mechanism for CO_2 control of stomatal movements.

RESULTS

Expression of YFP-Tagged βCA1 in Chloroplasts Rescues the Insensitive Stomatal Responses of *ca1ca4* Plants to CO_2 Changes

To characterize the cellular locations of βCA1 and βCA4 and gain insight into the sites of CO_2 responsiveness in guard cells, we generated transgenic *ca1ca4* plants expressing YFP fused to the C terminus of βCA1 or βCA4. These constructs were targeted to mature guard cells using the guard cell promoter *pGC1* (Yang et al., 2008). Analyses of nonguard cells in leaves, including epidermal pavement cells and mesophyll cells, showed no clear YFP fluorescence for the YFP fusion lines used for further analyses. Confocal microscopy analyses showed that YFP-tagged CA1 was targeted to the chloroplasts of guard cells (Fig. 1A), but no clear signal was detected in other compartments and locations in guard cells in leaves from more than 200 plants.

Previous research showed that βCA1 targeted mainly to chloroplasts upon expression in tobacco leaves (Fabre et al., 2007); however, a fraction of βCA1 expressed in tobacco leaves was also found at the plasma membrane (Hu et al., 2010). To further investigate this difference, we expressed different portions of βCA1 fused to YFPs in tobacco leaves. Biochemical studies of pea (*Pisum sativum*) CA had previously identified cleavage of the chloroplast targeting sequence at two different sites, resulting in two different protein lengths (Johansson and Forsman, 1992). The respective predicted cleavage sites are located before and after a highly charged region of the protein corresponding to amino acid 107 in βCA1 (Johansson and Forsman, 1992). We analyzed the protein sequences of βCA1 expressed in tobacco leaves by western blot and identified a prominent protein band with an apparent M_r of 25 kD (Fig. 2A). Additional analysis by tandem mass spectroscopy identified peptides starting from approximately amino acid 108. This indicates cleavage of βCA1 approximately upstream of amino acid 108 in a highly charged region consisting of seven acidic and five basic residues, which was similarly described for pea CA (Fig. 2B).

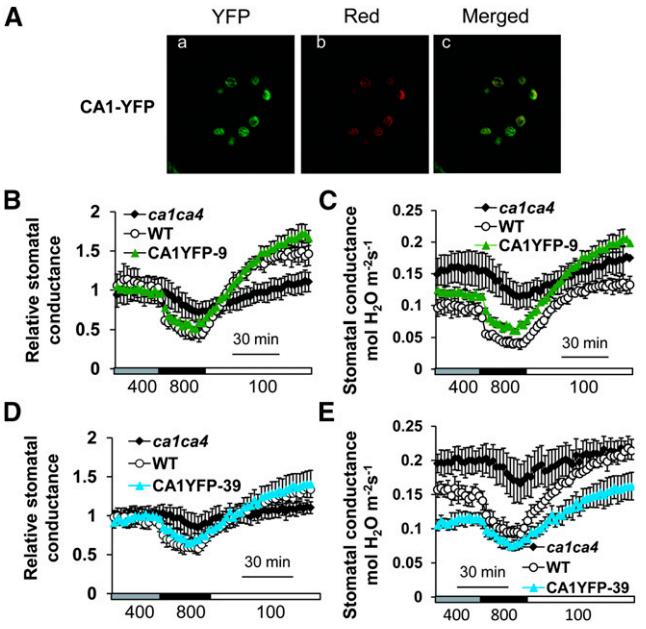

Figure 1. Chloroplast targeting of βCA1 restores CO_2 responsiveness when expressed in *ca1ca4* mutant guard cells. A, Confocal images showing CA1-YFP localization in chloroplasts of *ca1ca4* guard cells of line CA1YFP-9. Aa, CA1-YFP fusion proteins. Ab, Red chloroplast autofluorescence. Ac, Merged images. B to E, Time-resolved stomatal conductance responses to [CO_2] changes in two independent CA1-YFP-expressing lines in the *ca1ca4* background together with the wild type (WT) and *ca1ca4* mutant controls. Ambient CO_2 concentrations are shown below traces in microliters per liter in all gas exchange figure panels. Absolute stomatal conductance data are shown in C and E, and their corresponding relative stomatal conductance data are shown in B and D. $n = 4$ for each genotype. Data represent mean ± SEM.

Microscopic analysis of YFP-tagged βCA1 showed that the N terminus spanning the first 65 amino acids of βCA1 containing the chloroplast peptide signal was targeted to chloroplasts, whereas expression of a truncated βCA1 without the first 65 amino acids ($CA1_{66–330}$) was localized in the vicinity of the plasma membrane or cytoplasm (Fig. 3). These data suggest that, in tobacco plants, βCA1 could be cleaved, which results in the partial cytoplasm/plasma membrane localization of βCA1 in this system (Hu et al., 2010). Expression in tobacco may thus lead to mistargeting of some of the cleaved βCA1 protein.

We investigated whether the YFP-tagged βCA1 protein expressed in native guard cell chloroplasts in *ca1ca4* plants can complement the reduced CO_2 response phenotype of *ca1ca4* double-mutant plants. Gas exchange analyses in three independent transgenic lines showed complementation of the *ca1ca4* double mutant (Fig. 1, B–E).

Expression of YFP-Tagged βCA4 at the Plasma Membrane Rescues the Insensitive Stomatal Responses of *ca1ca4* to CO_2 Changes

In contrast to CA1-YFP, YFP-tagged βCA4 was detected at the plasma membrane of *ca1ca4* guard cells

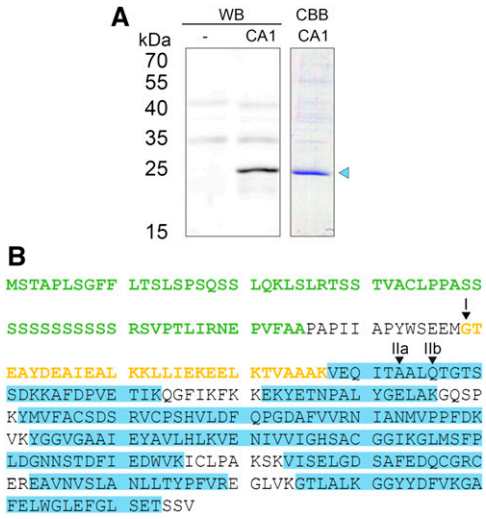

Figure 2. Western-blot (WB) and tandem mass spectrometry analyses of *βCA1* expressed in tobacco. A, WB of total protein extract from tobacco expressing p19-silencing inhibitor (lane 1) or p19-silencing inhibitor plus βCA1-StrepII (lane 2). βCA1-StrepII was purified from this extract and analyzed by Coomassie Brilliant Blue (CBB) staining (lane 3). The band representing cleaved βCA1-StrepII (blue triangle) was further analyzed by tandem mass spectrometry. B, Tandem mass spectrometry analysis of βCA1. The highly charged region at the N terminus is marked in yellow, and the chloroplast transit peptide is in green. Homologous sites to the cleavage site in pea CA are marked as I and II, with two different sites identified for II (Johansson and Forsman, 1992). Gels in A were run in separate experiments.

(Fig. 4A), consistent with transient expression in tobacco cells (Fabre et al., 2007; Hu et al., 2010). The CO_2 responses of βCA4-YFP-expressing transgenic lines were also complemented by the guard cell plasma membrane-localized βCA4-YFP in three independent lines (Fig. 4, B–E). Interestingly, these findings suggest that the βCA1-YFP and βCA4-YFP fusion constructs are functional, although these βCAs have distinct cellular sites of activity. These results show that the localization of βCA4 at the plasma membrane is sufficient to mediate CO_2-induced stomatal closing.

The above findings show that βCA1 and βCA4 localize to different cellular compartments in guard cells but that their expression regulates CO_2-induced stomatal movements. We therefore investigated whether mistargeting of βCA4 to chloroplasts would result in functional CO_2-regulated stomatal movements in *ca1ca4* guard cells. For mistargeting βCA4 to chloroplasts, the chloroplast transit peptide comprising the 55 N-terminal residues of the CHLOROPLAST-LOCALIZED IRON-SULFUR CLUSTER ASSEMBLY-LIKE PROTEIN (CpIscA) protein (Abdel-Ghany et al., 2005) was fused to βCA4-GFP, and the construct was driven by the guard cell promoter *pGC1* (Yang et al., 2008; Supplemental Fig. S1A). Confocal imaging analyses confirmed that βCA4-GFP was expressed in guard cell chloroplasts (Supplemental Fig. S1B). Three randomly selected independent transgenic ΔCplscA-CA4-GFP-expressing lines mistargeting βCA4 to chloroplasts in the *ca1ca4* background were chosen for analyses of CO_2 regulation of stomatal conductance. Notably, none of the investigated lines exhibited complete wild-type CO_2 responses (Supplemental Fig. S1, C–H). An apparent putative average weak recovery of the CO_2 response was observed in the ΔCplscA-CA4-GFP-12 line. However, this CO_2 response was not significant for the first 30 min after CO_2 was shifted to 100 $\mu L\ L^{-1}$ (Supplemental Fig. S1G; $P = 0.06$ compared with the wild type and $P = 0.88$ compared with *ca1ca4* plants).

The Phenotype of *ca1ca4* Plants Was Recovered by YFP-Tagged Human αCAII Expression in Cytosol and Nuclei

Previous data showed that a structurally unrelated human αCAII without YFP fusion also restored the stomatal response of *ca1ca4* to [CO_2] shifts (Hu et al., 2010). However, the cellular targeting of this unrelated αCAII was not resolved. We investigated the cellular targeting and in parallel, stomatal CO_2 responses in plants expressing YFP-tagged human αCAII. First, we transiently expressed the human CAII-YFP fusion construct in tobacco epidermal cell protoplasts. YFP signals were detected in both cytoplasm and the nuclear region and did not overlap with chlorophyll fluorescence of chloroplasts (Fig. 5, Ad–Af). Second, the

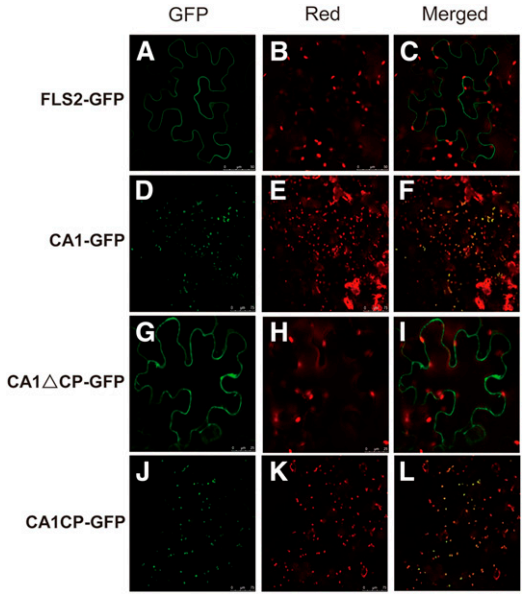

Figure 3. Subcellular localization of GFP fused to different deletions of βCA1 in transiently transformed tobacco epidermes. CA1-GFP is the full-length βCA1 protein fused to GFP that localizes to chloroplasts. CA1ΔCP-GFP is the GFP-fused βCA1 protein with the first 65 amino acids truncated, which includes a sequence from the chloroplast signal peptide. CA1CP-GFP represents the first 65 amino acids only containing chloroplast signal peptide sequence of βCA1 fused to GFP that expresses in chloroplasts. FLAGELLIN-SENSING2 (FLS2) was used as a control plasma membrane protein. A, D, G, and J, GFP. B, E, H, and K, Chloroplast autofluorescence. C, F, I, and L, Merged images.

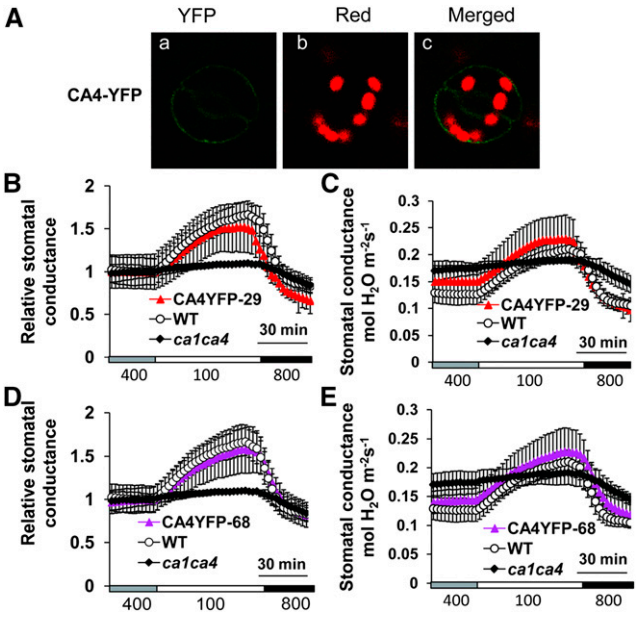

Figure 4. Plasma membrane targeting of βCA4 restores CO_2 responsiveness when expressed in *ca1ca4* mutant guard cells. A, Confocal images showing CA4-YFP localization at the plasma membrane of *ca1ca4* guard cells of line CA4YFP-68. Aa, YFP; Ab, red chlorophyll autofluorescence; Ac, merged image. B to E, Time-resolved stomatal conductance in two independent CA4-YFP-expressing *ca1ca4* lines and control plants. Absolute stomatal conductance data are shown in B and D, and their corresponding relative stomatal conductance data are shown in C and E. $n = 4$ for each genotype. Data represent mean ± SEM. WT, Wild type.

YFP-tagged human αCAII was expressed in *ca1ca4* guard cells using the *pGC1* promoter. The YFP-tagged human αCAII was detected in the cytoplasm and nucleus of guard cells (Fig. 5, Ah–Aj), similar to its expression in tobacco epidermal cells.

Stomatal conductance changes in response to CO_2 changes were determined in randomly selected human αCAII-YFP-expressing *ca1ca4* transgenic lines. Notably, human αCAII-YFP expression also rescued the stomatal responses to CO_2 changes of *ca1ca4* mutant plants (Fig. 5, B–E). These data suggest that the activities of human αCAII-YFP fusion proteins in the cytoplasm and nucleus are sufficient for regulation of stomatal CO_2 responses. Remarkably, together, all of these findings show that the investigated CAs are targeted to distinct cellular sites but retain, each one separately, the ability to complement the *ca1ca4* double mutant.

Compartmental Model for CO_2 Influx in Guard Cells Supports the Function of CAs in CO_2 Regulation of Stomatal Movements

To explore the above findings and the potential signaling components in CO_2 regulation of the stomatal closing pathway, we constructed a simplified model for the catalytic activity of CAs targeted to different compartments. We developed a compartmental mathematical model using parameters from a recent study on CO_2 influx into *Xenopus laevis* oocytes (Somersalo et al., 2012), which was modified to accommodate the much smaller cell size of guard cells. This model describes the interconversion of CO_2, HCO_3^-, and protons. Initially, we modeled the guard cell as a single compartment with spatially uniform concentration of reactants. This simplification was chosen given the small size of guard cells (approximately 10 μm) together with the large diffusion constants of the reactants CO_2 and HCO_3^-. We incorporated CA-like activity by multiplying the rate constants k_1 and k_{-1} (equations in "Materials and Methods") by an acceleration

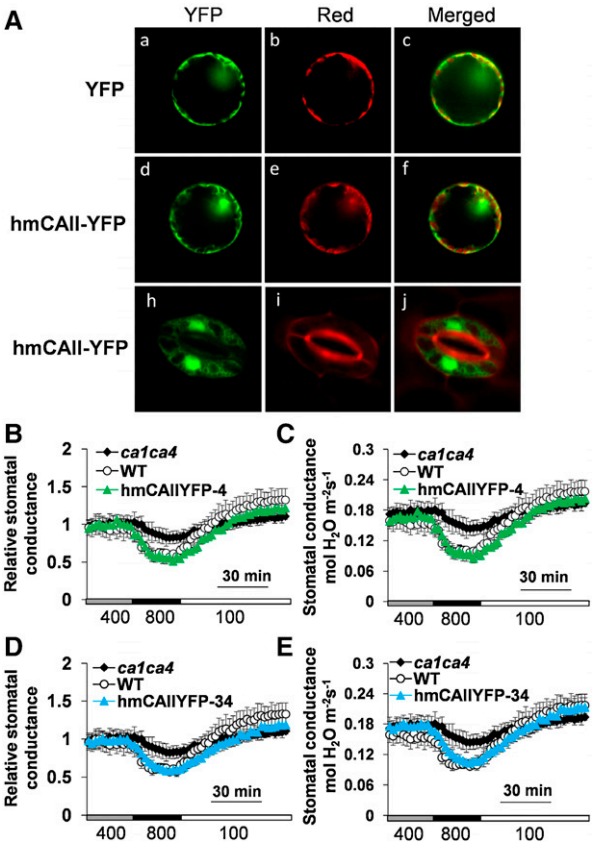

Figure 5. YFP-tagged human αCAII in guard cell cytoplasm and nucleus rescues the CO_2 responsiveness of the *ca1ca4* double mutant. A, Subcellular localization analyses of human αCAII-YFP in transiently transformed tobacco epidermal protoplasts and stably transformed guard cells of *ca1ca4* plants. Aa to Af, Confocal image analyses in tobacco epidermal protoplasts. Ah to Aj, Confocal images of human αCAII-YFP-expressing transgenic *ca1ca4* guard cells stained with FM4-64 ([*N*-{3-triethylammoniumpropyl}-4-{6-(4-[diethylamino]phenyl) hexatrienyl}pyridinium dibromide]). Aa, Ad, and Ah, YFP. Ab and Ae, Red chloroplast autofluorescence. Ai, Red fluorescence by FM4-64. Ac, Af, and Aj, Merged images. B to E, Time-resolved relative stomatal conductance in two independent human CAII-YFP-expressing *ca1ca4* lines and control plants. Absolute stomatal conductance data are shown in C and E, and their corresponding relative stomatal conductance responses are shown in B and F. $n = 4$ for each genotype. Data represent mean ± SEM. WT, Wild type.

factor A as described in the work by Somersalo et al. (2012). The starting condition for the simulation was at a CO_2 concentration (C_i) of 200 μL L^{-1} for both the leaf and the intracellular fluid (ICF), consistent with directly measured C_i values in leaves during the light period (Hanstein et al., 2001). A change of C_i to 800 μL L^{-1}, similar to leaves exposed to darkness (Hanstein et al., 2001), results in an influx of CO_2 into the cell, such that the internal CO_2 concentration rapidly approaches the external value. The simulated intracellular HCO_3^- concentration was plotted as a function of time in the presence and absence of CAs (Somersalo et al., 2012). In the presence of CAs, an acceleration factor of $A = 5$ was assumed for CO_2 dissociation in the cell (Somersalo et al., 2012; Fig. 6A, black curve; $A = 5$, with CA activity). In the absence of CA activity ($A = 1$), the predicted increase in the intracellular bicarbonate concentration occurred on a substantially slowed timescale (Fig. 6A, red curve; $A = 1$, without CA). Clearly, the presence of CAs ($A > 1$) changes the time course of the predicted bicarbonate concentration increase (Fig. 6A). Because elevated intracellular bicarbonate elevation causes stomatal closure

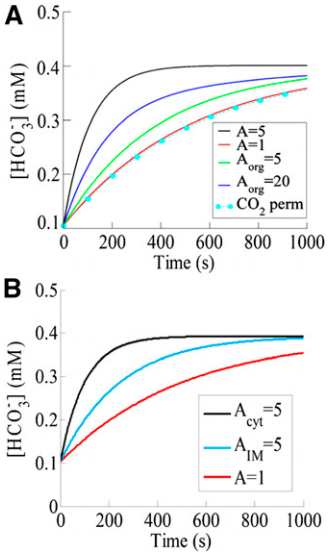

Figure 6. Computer simulations of HCO_3^- dynamics. A, Simulated intracellular HCO_3^- concentration as a function of time with CA activity (black curve) and without CA activity (red curve) in a compartmental model of a single guard cell. The increase in external CO_2 from 200 to 800 μL L^{-1} at time zero and the prior equilibrated internal (200 μL L^{-1}) CO_2 concentration at time zero lead to an influx of CO_2 into the cell. The presence of CAs results in faster dynamics of intracellular HCO_3^- concentration changes. Also shown is the simulated HCO_3^- concentration in the cytosol in a two-compartment model that includes an organelle (i.e. chloroplast) with two different CA-like activities (green curve, $A_{org} = 5$; and blue curve, $A_{org} = 20$) that is permeable to all components. The HCO_3^- dynamics for an organellar membrane ($A_{org} = 20$ and $A = 1$) that is only permeable to CO_2 are shown as cyan symbols (CO_2 perm). B, Simulated HCO_3^- concentration as a function of time using a spatial reaction-diffusion model of a cell. Shown are the dynamics with CA-like activity ($A = 5$) implemented everywhere in the cytosol (black curve), at the inner leaflet of the plasma membrane (cyan curve), and without any CA activity (red curve; $A = 1$).

and activates S-type anion channels in guard cells (Hu et al., 2010; Xue et al., 2011), the predicted time courses of [bicarbonate] change correlate with the slowed stomatal response to [CO_2] shifts in *ca1ca4* mutant plants. Note also that the steady-state value of the system is independent of the acceleration factor and thus, eventually, stomata may be predicted to be close to a similar level in *ca1ca4* mutant plants, albeit at a slower rate. This result can be explained by noting that, in a theoretical system that behaves as a closed system to all solutes other than CO_2, the CO_2/HCO_3^- buffering power in the steady state does not depend on the presence of CA. Thus, the results of our simulations could potentially explain the phenotype of stomatal movements observed in *ca1ca4* guard cells (Hu et al., 2010).

To determine the effects of CA localization for driving intracellular bicarbonate concentration changes, we have also simulated a small internal compartment representing an organelle, such as the chloroplast, within a larger compartment that corresponds to the guard cell. The acceleration factor in the guard cell's cytosol of *ca1ca4* mutant plants was taken to be one, whereas within the organelle, A_{org} was varied. Our simulations revealed that, for a chloroplast with an inner envelope membrane that does not permit substantial HCO_3^- release from the organelle back into the cytoplasm, the time course of cytosolic HCO_3^- concentration is largely unaffected (not accelerated) by the presence of organellar CA (Fig. 6A, cyan). The slight reduction in cytosolic HCO_3^- compared with $A = 1$ (Fig. 6A) can be understood by realizing that, because of the organellar CA, the chloroplast acts as a small sink for cytosolic CO_2, resulting in a marginally smaller cytosolic CO_2 and thus, a slightly slower production of cytosolic HCO_3^-.

Even assuming a chloroplast inner envelope membrane that is permeable to all components, including HCO_3^- flux from the chloroplast into the cytoplasm and choosing $A_{org} = 5$ resulted in cytosolic HCO_3^- dynamics that are considerably slower than those in our single-compartment model (compare the black and green curves in Fig. 6A). However, increasing the value of the organellar acceleration factor A_{org} is equivalent to choosing a CA with a larger activity in the organelle and will speed up this dynamics. We have verified this through explicit simulations that the predicted time course of HCO_3^- can be made similar to the one obtained using a single compartment with $A = 5$, if the organellar CA has a larger activity (blue curve in Fig. 6A; $A_{org} = 20$). These predictions may explain our experimental findings that the mistargeting of βCA4 to chloroplasts cannot complement the insensitive stomatal responses to CO_2 changes of the *ca1ca4* mutant (Supplemental Fig. S1), whereas at the plasma membrane, the βCA4 activity is sufficient. Furthermore, because it seems unlikely that the chloroplast membrane permits large rates of HCO_3^- or H_2CO_3 efflux from the chloroplast back to the cytoplasm, it also suggests that the role of organellar βCA1 might be more complex than simulated in our simple compartmental

model (Fig. 6A; A_{org} = 5 or 20). This view is also supported by our additional simplified simulation assuming no efflux of HCO_3^- from chloroplasts to the cytoplasm (Fig. 6A, cyan) and that chloroplasts have an important, yet to be identified contribution to CO_2 regulation of stomatal movements (see "Discussion").

Reaction-Diffusion Model of CO_2 Influx into Guard Cells Can Explain the Effect of CA Localization for Regulation of Stomatal Movements

To investigate further the effect of CA localization for driving intracellular HCO_3^- concentration changes, we used a distinct full spatial reaction-diffusion mathematical model, as reported by Somersalo et al. (2012), appropriately modified to represent a single cell of guard cell dimension surrounded by the bulk extracellular cell wall space (for details, see "Materials and Methods"). Unlike the simplified compartmental model described above, this model accounts for spatial variability and allows for the implementation of CA-like activity at the inner leaflet of the plasma membrane. As before, we allowed the system to reach equilibrium at a low C_i and then increased the CO_2 concentration as described in "Materials and Methods." Figure 6B illustrates the predicted intracellular HCO_3^- concentration as a function of time for a simulation in which CA activity (A_{cyt} = 5) is implemented everywhere inside the cell (Fig. 6B, black curve; cytoplasm) or only at the plasma membrane (Fig. 6B, cyan curve; A_{IM} = 5). As a control, we have also plotted the time course of the HCO_3^- concentration for a simulation in which no CA-like activity is implemented (A = 1; red curve in Fig. 6B). Note that each curve corresponds to the concentration at a depth of approximately 5 μm into the cell. We have verified that this spatial model predicts virtually identical dynamics of HCO_3^- concentration changes at any depth into the cell. This can be explained because of the small size of guard cells and the large diffusion rates of the reactants inside the cell (see above).

Consistent with the single-compartment model of a guard cell (Fig. 6A), in the absence of CA-like activity, intracellular HCO_3^- concentration rises very slowly, whereas in the presence of CA-like activity, the production of HCO_3^- occurs at a faster rate and therefore, results in faster dynamics of HCO_3^- concentration changes. When CA-like activity is implemented everywhere in the cytosol (A_{cyt} = 5; black curve in Fig. 6B), the rise in HCO_3^- concentration is faster than when CA-like activity is implemented only at the inner leaflet of the plasma membrane (Fig. 6B, cyan curve; A_{IM} = 5). This difference in rates of HCO_3^- concentration changes predicted in this simplified model occurs, because when CA-like activity is implemented everywhere in the cell, there is a rapid consumption of incoming CO_2 at every location within the cell, whereas when CA-like activity is implemented only at the inner leaflet of the plasma membrane, this conversion occurs only near the plasma membrane. Nevertheless, the HCO_3^- concentration in the presence of membrane-bound CAs increases faster than in the absence of any CA-like activity. Moreover, this increase could be even faster by assuming an even larger CA activity at the membrane.

One prediction of the above model, assuming that HCO_3^- is the intracellular signal that transmits the CO_2 response (Xue et al., 2011; Tian et al., 2015), is that longer exposures to elevated CO_2 should enable stomata of *ca1ca4* mutant plants to close to similar levels as wild-type plants but at a slowed rate. Because the rate of stomatal closing was found previously to be slowed in *ca1ca4* mutant plants (Hu et al., 2010), we conducted experiments in which prolonged elevated CO_2 concentrations were applied. The stomatal conductance of *ca1ca4* mutant plants was reduced to a similar level compared with wild-type plants when CO_2 was increased from 400 to 800 μL L^{-1} for more than 90 min under the imposed conditions (Fig. 7). These findings also point to secondary compensatory feedback mechanisms that may strengthen the response to CO_2 shifts in *ca1ca4* plants due to the enhanced stomatal conductance (Hu et al., 2010; Engineer et al., 2014). These experiments suggest that, if the starting CO_2 concentration is 400 μL L^{-1} and the CO_2 concentration is rapidly increased to 800 μL L^{-1} for prolonged exposures, stomata eventually can close to similar or even lower levels than wild-type plants.

DISCUSSION

This study investigates the cellular localizations of CAs in guard cells and the roles that these distinct CA enzymes play in regulating rapid stomatal conductance changes in response to CO_2 concentration changes. Interestingly, use of fluorescently tagged CAs here shows that targeting of either native βCA4 to the plasma membrane or βCA1 to the chloroplast is sufficient for recovering CO_2 responses (Fig. 1). However, when ΔCplscA-CA4-GFP was experimentally targeted to chloroplasts, the stomatal CO_2 response was not restored (Supplemental Fig. S1). It is conceivable that the precise targeting within chloroplast compartments of CAs is essential or that the CA activity of this fusion

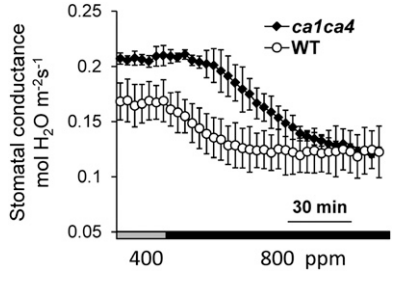

Figure 7. Stomatal conductance of *ca1ca4* plants to a stepped increase and long exposure to high CO_2. Stomatal conductance analyses of *ca1ca4* and wild-type (WT) plants in response to a step to high CO_2 for a long exposure (120 min). n = 4 leaves for each genotype.

protein was diminished. Consistent with these results, previous membrane proteomic studies in Arabidopsis (Froehlich et al., 2003; Kawamura and Uemura, 2003) and transient expression in tobacco (Fabre et al., 2007; Hu et al., 2010) indicated that βCA1 is expressed in chloroplasts, with a small fraction of cleaved βCA1 protein detected at the plasma membrane or in the cytoplasm upon transient overexpression in tobacco leaves (Figs. 2 and 3), and that βCA4 localizes at the plasma membrane. The mechanism mediating βCA4 localization at the plasma membrane will require further research. Here, we show that both of these distinct cellular locations are sufficient to restore CO_2 signal transduction.

The findings that *ca1ca4* double-mutant leaves produce a considerably slowed CO_2 response in rapid CO_2-controlled stomatal movements together with complementation of this phenotype for either of the differential native localizations of the βCA1 and βCA4 (Figs. 1 and 4) suggest relevant and unique roles for βCA1 and βCA4 in the CO_2 response. The two mathematical models applied here may explain these unexpected findings. Active CAs modeled in a small cell of guard cell dimensions are predicted to accelerate the bicarbonate dynamics in the cytosol and accelerate CO_2 flux into guard cells (Fig. 6), thus inducing stomatal movement responses. Furthermore, modeling of CA activity at the plasma membrane or in the cytosol suggests that either activity should be able to accelerate increases in HCO_3^- concentration in guard cells (Fig. 6B). It is interesting that plasma membrane and chloroplast overexpression localizations both complement the mutant. The simplified models thus predict that the intermediate rates of HCO_3^- production at the plasma membrane relative to a bulk cytoplasmic location are sufficient for the biological response. The prediction that HCO_3^- increases are not highly sensitive to the precise location of CAs, at the plasma membrane or in the cytoplasm, is consistent with the small dimensions of guard cells and the rapid diffusion rates of bicarbonate in solution. Any spatial separation of reactants at the inner leaflet of the plasma membrane or in the bulk cytosol will thus equilibrate rapidly. These predictions correlate with the complementation data found here for distinct cellular localizations of CAs at the plasma membrane (Fig. 4) or in the cytoplasm (Fig. 5) and would support a model in which the intracellular bicarbonate concentration is a mediator of stomatal closing.

Mathematical modeling also predicted that, after long CO_2 exposures, wild-type and CA mutant stomata should reach similar HCO_3^- concentrations and thus, possibly stomatal apertures, albeit at slower rates in CA mutant leaves. When steps to 800 $\mu L\ L^{-1}$ were applied for 120 min, stomatal conductance of both genotypes reached similar levels (Fig. 7). This was unexpected, because *ca1ca4* leaves have a higher stomatal density and index than wild-type leaves, including in mature leaves (Engineer et al., 2014) used here for gas exchange analyses. Thus, findings from long CO_2 pulses further indicate that the response to CO_2 steps maybe partially up-regulated in *ca1ca4* mutants as a secondary compensatory feedback mechanism in *ca1ca4* mutant plants. A compensatory response of stomatal conductance was recently identified in *slac1* mutants (Laanemets et al., 2013). Additional research will be needed to investigate possible secondary compensatory feedback response mechanisms in stomatal movement mutants.

Additional mathematical modeling suggests that CAs confined to small intracellular organelles, such as chloroplasts, are not as effective in accelerating the dynamics of cytoplasmic [HCO_3^-] as those localized either at the inner leaflet of the plasma membrane or in the cytosol (Fig. 6A). This principle may partially explain why βCA4 expressed in chloroplasts could not complement the CO_2-insensitive stomatal responses in *ca1ca4* mutant leaves, whereas βCA4 at the plasma membrane could. Chloroplastic βCA1 activity may be larger than mistargeted chloroplast βCA4 activity. Analysis of biochemical CA activities in the wild type, *ca1* and *ca4* single-mutant plants, and *ca1ca4* double-mutant plants has previously shown that βCA1 accounts for 80% of the catalytic CA activity in planta (Hu et al., 2010). In contrast, *βCA4* mutation had a limited effect on the overall catalytic CA activity in planta (Hu et al., 2010). Thus, the complementation by the chloroplast-targeted βCA1 is presumably because of some combination of a higher catalytic activity or a higher protein density compared with βCA4. Note also that we may have mistargeted βCA4 to the improper chloroplast compartment.

The simplified intracellular compartment modeling pursued here indicates that the function of βCA1 in chloroplasts may not simply be to accelerate the rate of cytosolic [HCO_3^-] increase at elevated CO_2. Furthermore, chloroplasts are expected not to easily permit substantial rates of release of bicarbonate from the chloroplast stroma back into the cytoplasm in the presence of a highly active CA, such as βCA1. This is exemplified in the extreme (boundary condition) model assuming that the inner chloroplast envelope membrane does not permit HCO_3^- release (Fig. 6A, cyan). Thus, an additional yet to be identified chloroplast function of βCA1 is predicted to be required in the rapid CO_2 control of stomatal movements.

This study does not exclude an additional important function of βCA1 in chloroplasts in addition to a possible contribution to mediating acceleration of the dynamics of intracellular HCO_3^- concentration changes in guard cells. Chloroplast reactions and a chloroplast HCO_3^--CO_2 sink may contribute to the CO_2 responses by enhancing the plasma membrane cellular influx of CO_2-HCO_3^- into guard cells, and additional research will be needed to investigate putative chloroplast contributions to the CO_2 response. Note that guard cell chloroplast functions during CO_2 control of stomatal movements may be independent of Rubisco (von Caemmerer et al., 2004) and are not dependent on guard cell photosynthesis (Azoulay-Shemer et al., 2015). Guard cell chloroplasts could function in malate-starch interconversion during stomatal movements (Outlaw and Manchester, 1979).

Recent findings in maize show that ZmCA1 and ZmCA2 are not limiting for photosynthesis at current ambient CO_2 concentrations, but these cytoplasm-targeted CAs function in CO_2 flux and maintenance of high rates of photosynthesis when CO_2 availability is limiting (Studer et al., 2014). Targeting of the highly active human αCAII (Kern et al., 1995; Hu et al., 2010) is sufficient to restore CO_2 control of stomatal conductance, despite being targeted to the guard cell cytoplasm (Fig. 5). These findings are consistent with the CO_2-HCO_3^- model, because the cytoplasmic CA activity would be predicted to cause an accelerated increase in the HCO_3^- concentration in the cytoplasm (Fig. 6), which in turn, is known to be required for high CO_2-activated S-type anion channels in guard cells (Xue et al., 2011; Tian et al., 2015). Furthermore, a large cytoplasmic human αCAII activity may also enhance the flux of CO_2-HCO_3^- across the plasma membrane to chloroplasts and other possible intracellular CO_2-HCO_3^- sinks.

In summary, this study shows that the cellular location of three distinct CA proteins differs in guard cells, at the plasma membrane, in the cytoplasm, and in chloroplasts, but interestingly, these three locations are sufficient for mediating CO_2 control of gas exchange in plants. Mathematical modeling suggests that CA-induced acceleration of changes in the intracellular bicarbonate concentration rather than cellular CO_2-HCO_3^- flux alone is an important mechanism for CO_2 control of stomatal movements and that this mechanism can be achieved by distinct cellular locations of CAs. An additional mathematical model indicates that guard cell chloroplasts have an additional yet to be identified function in CO_2 control of stomatal movements that will require further investigation.

MATERIALS AND METHODS

Plant Growth and Genotypes

Arabidopsis (*Arabidopsis thaliana*) plants used in this study were Columbia-0 ecotype and grown in a Conviron Growth Chamber at 21°C with 60% to 80% humidity and a 16-h-light/8-h-dark photoperiod regime at approximately 75 μmol m^{-2} s^{-1}. The isolation of the βCA *ca1ca4* double mutant was as described in the work by Hu et al. (2010).

YFP-Tagged CA Constructs and Expression in *ca1ca4*

For YFP-tagged expression of *βCA1*, *βCA4*, and human *CAII*, complementary DNAs in guard cells of *ca1ca4*, *βCA1*, *βCA4*, and human *CAII* were amplified and recombined into the binary vector pXC27G-YFP, which was derived from pXCSG-YFP (Feys et al., 2005). The 35S promoter was replaced by the mature guard cell-preferential promoter *pGC1* (Yang et al., 2008). *βCA1* was amplified by primers CA1F (5′-ggggacaagtttgtacaaaaaagcaggctatagtagcttccataagagtc-3′) and CA1R (5′-ggggaccactttgtacaagaaagctgggtcaagtccccaaagctcaaa-3′). *βCA4* was amplified by primers CA4F (5′-ggggacaagtttgtacaaaaaagcaggctaatggctcctgcattcgg-3′) and CA4R (5′-ggggaccactttgtacaagaaagctgggtaggcaaaagcaggagtg-3′). Human *CAII* was amplified by primers CAIIF (5′-ggggacaagtttgtacaaaaaagcaggctcgaccatgtcccatcact-3′) and CAIIR (5′-ggggaccactttgtacaagaaagctgggttttgcctgttcttcagtg-3′) from the complementary DNA clone SC107902 (OriGENE; Hu et al., 2010). For targeting CA4 to guard cell chloroplasts in *ca1ca4* mutant plants, the construct ΔCpIscA-CA4-GFP in a modified pGreen vector driven by the mature guard cell-preferential promoter *pGC1* (Yang et al., 2008) was created. CA4 was amplified by primers CA4F2 (5′-aactgcagaatggctcctgcattcgg-3′; with *Pst*I adapter) and CA4R2 (5′-aaggatccaggcaaaagcaggagtg-3′; with *Bam*HI adapter) and fused to GFP in the vector pGreen-pGC1-GFP at the sites of *Pst*I and *Bam*HI to create the construct pGreen-pGC1-CA4-GFP. ΔCpIscA, the 55 N-terminal amino acids of the chloroplast-localized CpIscA protein (Abdel-Ghany et al., 2005), was amplified by ΔCpIscAF (5′-aaccatggcgcatttgaatcagcaga-3′; with *Nco*I adapter) and ΔCpIscAR (5′-aactgcaggaagcggatcgaacagaaa-3′; with *Pst*I adapter) and fused to CA4-GFP at the sites of *Nco*I and *Pst*I in the construct. Constructs generated were transformed into *ca1ca4* plants by the floral dipping method (Clough and Bent, 1998).

Subcellular Localization Analyses of YFP-Tagged CA Proteins

To analyze the localization of different portions of *βCA1* in the tobacco (*Nicotiana benthamiana*) epidermis, the full length of *βCA1* was amplified by the primers CA1-F (5′-ggggacaagtttgtacaaaaaagcaggctatgtcgaccgctcctctctc-3′) and CA1-R (5′-ggggaccactttgtacaagaaagctgggtacagcttccaatgtagtatggtagcc-3′) and fused to GFP in the vector barII_pUBQ10_GFPc-GWB (provided by Jorg Kudla) as CA1-GFP. CA1ΔCP-GFP is the βCA1 protein with the first 65 amino acids deleted. It is amplified by CA1 (NDel)-F (5′-ggggacaagtttgtacaaaaaagcaggctcctgctcctatcattgcccc-3′) and CA1-R and fused to GFP; CA1CP-GFP represents the first 65 amino acids of βCA1 amplified by CA1-F and CA1-R(Del) (5′-ggggaccactttgtacaagaaagctgggtaagcggcaaaaactggctcgtt-3′) fused to GFP. To transiently express human CAII-YFP in the tobacco epidermis, the human CAII amplified by primers CAIIF2 and CAIIR2 was fused to YFP in the vector construct pXCSG-YFP (Feys et al., 2005). The pH35YG vector containing 35S::YFP was used as a positive control for cytoplasmic and nuclear localizations (Kubo et al., 2005). FLAGELLIN-SENSING2 is used as a control of membrane protein. Protoplasts were isolated from infiltrated leaves as described previously (Hu et al., 2010). For the localization of YFP-tagged CA1 and CA4 in *ca1ca4* guard cells, the leaf epidermal layers were directly imaged for YFP fluorescence using confocal microscopy. For YFP-tagged human CAII in *ca1ca4* guard cells, the leaf epidermal layers were first stained with FM4-64 for 10 min. Fluorescence imaging was acquired by spinning-disc confocal microscopy with an electron-multiplying CCD camera (CascadeII: 512; Photometrics) using Metamorph software (Universal Imaging).

Tandem Mass Spectrometry Analysis of βCA1

Transient transformation of 4-week-old tobacco plants and purification of βCA1-StrepII were performed as described (Witte et al., 2004). For SDS-PAGE, one volume of washed Macroprep beads were resuspended in one volume of 2× SDS-gel loading buffer and heated to 90°C for 6 min. Proteins were separated by SDS-PAGE and analyzed by Strep Tactin-alkaline phosphatase conjugate (IBA) as described (Witte et al., 2004). Tryptic digestion of StrepII-purified proteins was performed in gel. Proteins were reduced with 10 mM dithiothreitol at 56°C for 1 h and alkylated with 55 mM iodoacetamide at room temperature for 45 min. Proteins were digested using 0.4 μg of Trypsin Singles (Sigma Aldrich) at room temperature overnight. Digests were desalted for electrospray mass spectrometry with a C18 Reverse-Phase ZipTip Resin (Millipore). A QSTAR Elite Quadrupole-TOF Mass Spectrometer equipped with a Nano-Spray Source and nanoLC System (AB Sciex) was used for analysis. Resulting wiff files were converted into mzXML format and analyzed using PEAKS Studio 7.0. Database search was performed against The Arabidopsis Information Resource Database (TAIR10_pep_20101214) with a 0.1% false discovery rate cutoff. Carbamidomethylation was set as a fixed modification, and phosphorylation and Met oxidation were selected as variable modifications. Additional variable modifications were identified by PEAKS PTM software (Bioinformatics Solutions Inc.). Fragment ion tolerance was set to 0.1 D, and variable modifications per peptide were limited to three.

Time-Resolved Intact Leaf Gas Exchange Analyses

Gas exchange analyses were performed on rosette leaves from 5-week-old plants in response to the imposed leaf [CO_2] changes at 150-mmol m^{-2} s^{-1} light (Parabolic Aluminum Reflector) fluence rate using an Li6400XT Gas Exchange Analyzer fitted with a fluorimeter chamber (Li-Cor Inc.) as described in Hu et al., 2010. Stomatal conductance was first stabilized at ambient [CO_2] (400 μL L^{-1}) for 30 min; then, unless otherwise noted in the figures, [CO_2] was shifted to a high concentration (800 μL L^{-1}) for 30, 60, or 90 min and again changed to a low concentration (100 μL L^{-1}) for at least 30 min.

Alternately, $[CO_2]$ was held at the ambient CO_2 concentration for at least 30 min, shifted to a low concentration (100 μL L^{-1}), and then changed to a high concentration for indicated times noted in the figures. The data presented are means of at least three leaves per genotype per treatment ± SEM. Relative stomatal conductance values were determined by normalization relative to the average of 10 data points preceding the $[CO_2]$ transitions (400–800 μL L^{-1} or 400–100 μL L^{-1}).

Compartmental Model for CO_2 Influx in Guard Cells

A simplified model in guard cells for CO_2 catalysis was constructed by modification of a model examining CO_2 influx in oocytes (Somersalo et al., 2012). The model describes the formation and dissociation of carbonic acid as

$$CO_2 + H_2O \underset{k_{-1}}{\overset{k_1}{\rightleftarrows}} H_2CO_3 \underset{k_{-2}}{\overset{k_2}{\rightleftarrows}} HCO_3^- + H^+$$

along with a reaction describing a non-CO_2/HCO_3^- buffer

$$HA \underset{k_{-3}}{\overset{k_3}{\rightleftarrows}} A^- + H^+$$

where k_1, k_{-1}, k_2, k_{-2}, k_3, and k_{-3} are rate constants. We incorporated CA-like activity by multiplying the rate constants k_1 and k_{-1} by an acceleration factor A (Somersalo et al., 2012). We assumed that the membrane is permeable to CO_2 with a permeability constant P_m. The rate equations corresponding to the above reactions can be easily obtained. For example, for the CO_2 concentration, we have

$$\frac{dCO_2}{dt} = k_{-1}H_2CO_3 - k_1CO_2 + P_m(CO_2{}^{ext} - CO_2)$$

where $CO_2{}^{ext}$ is the external CO_2 concentration. The resulting set of equations was solved using an algorithm suitable for stiff ordinary differential equations using parameter values in Somersalo et al., 2012. As initial conditions, the initial internal and external CO_2 concentration were set to 200 μL L^{-1}, similar to CO_2 conditions measured in leaves exposed to light (Hanstein et al., 2001), whereas the internal and external pH levels were taken to be 7.4 and 6, respectively. Finally, the acceleration factor caused by CA activity was chosen to be five (Somersalo et al., 2012). At the start of the simulation, the external CO_2 concentration was set to 800 μL L^{-1}. For determining the effects of CA localization, a small internal compartment representing an organelle, such as the chloroplast taking up 10% of the cell volume within a larger compartment that corresponds to the guard cell, was simulated. The organelle membrane was modeled as being permeable to either all components or exclusively CO_2 using the same permeability constants as for the cell membrane. The acceleration factor within the compartment representing the *ca1ca4* mutant guard cell's cytosol was taken to be one, whereas this acceleration within the organelle, A_{org}, was varied.

Reaction-Diffusion Model of CO_2 Influx into Guard Cells

As a starting point, we used the above-mentioned reaction-diffusion model of CO_2 influx into a *Xenopus laevis* oocyte developed by Somersalo et al. (2012). This model assumes that the cell is a perfectly symmetric sphere surrounded by a thin layer of extracellular unconvected fluid (EUF), which in turn, is surrounded by the bulk extracellular fluid (BECF). In both EUF and ICF, the model accounts for the CO_2/HCO_3^- equilibrium, including the slow conversion of CO_2 into H_2CO_3 and vice versa, and a multitude of non-CO_2/HCO_3^- buffers. Solutes can diffuse within the EUF and ICF. The plasma membrane is infinitely thin and permeable to CO_2. The EUF, ICF, and the plasma membrane have properties of pure water. Mathematically, the changes of solute concentrations in time and space are described by a coupled system of partial differential equations, which are solved assuming spherical radial symmetry (i.e. solute concentrations depend only on the radial distance from the center of the cell). Numerically, the system of partial differential equations is solved using the method of lines with appropriate spatial discretization schemes, and the resulting system of ordinary differential equations is solved using the MATLAB stiff ode solver, ode15s. The details of the numerical implementation are provided in Somersalo et al., 2012. Here, we explain how we modified this model to account for guard cell dimensions and the experimental conditions in this study. We assumed that the guard cell is a sphere with a radius of 10 μm surrounded by a 5-μm-thick EUF. The EUF represents the aqueous solution in the space in the cell walls surrounding the guard cell. We assumed that the EUF contains only the CO_2/HCO_3^- buffer system but that the ICF contains both a CO_2/HCO_3^- buffer system and a single non-CO_2/HCO_3^- buffer. For diffusion constants, rate constants, and the properties of the intracellular non-CO_2/HCO_3^- buffer system, we used the values reported in Somersalo et al., 2012. As done in the work by Somersalo et al. (2012), we implemented CA-like activity by multiplying the rate constants k_{+1} and k_{-1} by the same acceleration factor A.

We performed each of the three simulations illustrated in Figure 6B in two steps. First, we exposed the guard cell ($[CO_2]_{ICF}$ = 0, pH_{ICF} 7.40) to a BECF-containing equilibrated CO_2/HCO_3^- ($[CO_2]_{BECF}$ = 200 μL L^{-1}, pH_{BECF} 6.00) and waited for the system to achieve equilibrium (i.e. $[CO_2]_{ICF}$ = $[CO_2]_{BECF}$ = 200 μL L^{-1}). We ran this first simulation for 10,000 s (data not shown). Second, we used the final state of this first simulation to define the intracellular composition of the guard cell and ran a second simulation, in which we shifted $[CO_2]_{BECF}$ from 200 to 800 μL L^{-1} and pH_{BECF} to 6.00. Figure 6B shows the second of these simulations.

Statistical Analyses

Data are represented as mean ± SEM unless otherwise noted. Comparisons between continuous variables were performed using the Student's *t* test with a two-tailed distribution and two-sample equal variance.

Sequence data from this article can be found in the GenBank/EMBL data libraries under accession numbers AT3G01500 for CA1 and AT1G70410 for CA4.

Supplemental Data

The following supplemental materials are available.

Supplemental Figure S1. Chloroplast mistargeted ΔCpIscA-CA4-GFP does not complement CO_2 responsiveness of the *ca1ca4* double mutant.

Received April 30, 2015; accepted July 28, 2015; published August 4, 2015.

LITERATURE CITED

Abdel-Ghany SE, Ye H, Garifullina GF, Zhang L, Pilon-Smits EA, Pilon M (2005) Iron-sulfur cluster biogenesis in chloroplasts: involvement of the scaffold protein CpIscA. Plant Physiol **138:** 161–172

Azoulay-Shemer T, Palomares A, Bagheri A, Israelsson-Nordstrom M, Engineer CB, Bargmann BOR, Stephan AB, Schroeder JI (2015) Guard cell photosynthesis is critical for stomatal turgor production, yet does not directly mediate CO_2- and ABA-induced stomatal closing. Plant J **83:** 567–581

Badger MR, Price GD (2003) CO_2 concentrating mechanisms in *cyanobacteria*: molecular components, their diversity and evolution. J Exp Bot **54:** 609–622

Cardon ZG, Berry JA, Woodrow IE (1994) Dependence of the extent and direction of average stomatal response in *Zea mays* L. and *Phaseolus vulgaris* L. on the frequency of fluctuations in environmental stimuli. Plant Physiol **105:** 1007–1013

Chandrashekar J, Yarmolinsky D, von Buchholtz L, Oka Y, Sly W, Ryba NJ, Zuker CS (2009) The taste of carbonation. Science **326:** 443–445

Clough SJ, Bent AF (1998) Floral dip: a simplified method for Agrobacterium-mediated transformation of *Arabidopsis thaliana*. Plant J **16:** 735–743

Cousins AB, Badger MR, von Caemmerer S (2008) C4 photosynthetic isotope exchange in NAD-ME- and NADP-ME-type grasses. J Exp Bot **59:** 1695–1703

DeLucia EH, Hamilton JG, Naidu SL, Thomas RB, Andrews JA, Finzi A, Lavine M, Matamala R, Mohan JE, Hendrey GR, et al (1999) Net primary production of a forest ecosystem with experimental CO_2 enrichment. Science **284:** 1177–1179

Engineer CB, Ghassemian M, Anderson JC, Peck SC, Hu H, Schroeder JI (2014) Carbonic anhydrases, EPF2 and a novel protease mediate CO_2 control of stomatal development. Nature **513:** 246–250

Fabre N, Reiter IM, Becuwe-Linka N, Genty B, Rumeau D (2007) Characterization and expression analysis of genes encoding alpha and beta carbonic anhydrases in *Arabidopsis*. Plant Cell Environ **30:** 617–629

Ferris KE, Clark RD, Coates EL (2007) Topical inhibition of nasal carbonic anhydrase affects the CO_2 detection threshold in rats. Chem Senses **32:** 263–271

Feys BJ, Wiermer M, Bhat RA, Moisan LJ, Medina-Escobar N, Neu C, Cabral A, Parker JE (2005) *Arabidopsis* SENESCENCE-ASSOCIATED GENE101 stabilizes and signals within an ENHANCED DISEASE SUSCEPTIBILITY1 complex in plant innate immunity. Plant Cell **17:** 2601–2613

Froehlich JE, Wilkerson CG, Ray WK, McAndrew RS, Osteryoung KW, Gage DA, Phinney BS (2003) Proteomic study of the *Arabidopsis thaliana* chloroplastic envelope membrane utilizing alternatives to traditional two-dimensional electrophoresis. J Proteome Res **2:** 413–425

Fukuzawa H, Fujiwara S, Yamamoto Y, Dionisio-Sese ML, Miyachi S (1990) cDNA cloning, sequence, and expression of carbonic anhydrase in Chlamydomonas reinhardtii: regulation by environmental CO_2 concentration. Proc Natl Acad Sci USA **87:** 4383–4387

Giordano M, Norici A, Forssen M, Eriksson M, Raven JA (2003) An anaplerotic role for mitochondrial carbonic anhydrase in *Chlamydomonas reinhardtii*. Plant Physiol **132:** 2126–2134

Hanstein S, de Beer D, Fellea HH (2001) Miniaturised carbon dioxide sensor designed for measurements within plant leaves. Sens Actuators B Chem **81:** 107–114

Hashimoto M, Negi J, Young J, Israelsson M, Schroeder JI, Iba K (2006) *Arabidopsis* HT1 kinase controls stomatal movements in response to CO_2. Nat Cell Biol **8:** 391–397

Hatch MD, Burnell JN (1990) Carbonic anhydrase activity in leaves and its role in the first step of C_4 photosynthesis. Plant Physiol **93:** 825–828

Hetherington AM, Woodward FI (2003) The role of stomata in sensing and driving environmental change. Nature **424:** 901–908

Hewett-Emmett D, Tashian RE (1996) Functional diversity, conservation, and convergence in the evolution of the alpha-, beta-, and gamma-carbonic anhydrase gene families. Mol Phylogenet Evol **5:** 50–77

Hu H, Boisson-Dernier A, Israelsson-Nordström M, Böhmer M, Xue S, Ries A, Godoski J, Kuhn JM, Schroeder JI (2010) Carbonic anhydrases are upstream regulators of CO_2-controlled stomatal movements in guard cells. Nat Cell Biol **12:** 87–93

Hu J, Zhong C, Ding C, Chi Q, Walz A, Mombaerts P, Matsunami H, Luo M (2007) Detection of near-atmospheric concentrations of CO_2 by an olfactory subsystem in the mouse. Science **317:** 953–957

Johansson IM, Forsman C (1992) Processing of the chloroplast transit peptide of pea carbonic anhydrase in chloroplasts and in Escherichia coli: identification of two cleavage sites. FEBS Lett **314:** 232–236

Kawamura Y, Uemura M (2003) Mass spectrometric approach for identifying putative plasma membrane proteins of *Arabidopsis* leaves associated with cold acclimation. Plant J **36:** 141–154

Kern G, Kern D, Schmid FX, Fischer G (1995) A kinetic analysis of the folding of human carbonic anhydrase II and its catalysis by cyclophilin. J Biol Chem **270:** 740–745

Kubo M, Udagawa M, Nishikubo N, Horiguchi G, Yamaguchi M, Ito J, Mimura T, Fukuda H, Demura T (2005) Transcription switches for protoxylem and metaxylem vessel formation. Genes Dev **19:** 1855–1860

Laanemets K, Wang YF, Lindgren O, Wu J, Nishimura N, Lee S, Caddell D, Merilo E, Brosche M, Kilk K, et al (2013) Mutations in the SLAC1 anion channel slow stomatal opening and severely reduce K^+ uptake channel activity via enhanced cytosolic $[Ca^{2+}]$ and increased Ca^{2+} sensitivity of K^+ uptake channels. New Phytol **197:** 88–98

Lane TW, Morel FM (2000) A biological function for cadmium in marine diatoms. Proc Natl Acad Sci USA **97:** 4627–4631

Lee M, Choi Y, Burla B, Kim YY, Jeon B, Maeshima M, Yoo JY, Martinoia E, Lee Y (2008) The ABC transporter AtABCB14 is a malate importer and modulates stomatal response to CO_2. Nat Cell Biol **10:** 1217–1223

Ludwig M (2012) Carbonic anhydrase and the molecular evolution of C4 photosynthesis. Plant Cell Environ **35:** 22–37

Medlyn BE, Barton CVM, Broadmeadow MSJ, Ceulemans R, De Angelis P, Forstreuter M, Freeman M, Jackson SB, Kellomaki S, Laitat E, et al (2001) Stomatal conductance of forest species after long-term exposure to elevated CO_2 concentration: a synthesis. New Phytol **149:** 247–264

Moroney JV, Ma Y, Frey WD, Fusilier KA, Pham TT, Simms TA, DiMario RJ, Yang J, Mukherjee B (2011) The carbonic anhydrase isoforms of *Chlamydomonas reinhardtii*: intracellular location, expression, and physiological roles. Photosynth Res **109:** 133–149

Negi J, Matsuda O, Nagasawa T, Oba Y, Takahashi H, Kawai-Yamada M, Uchimiya H, Hashimoto M, Iba K (2008) CO_2 regulator SLAC1 and its homologues are essential for anion homeostasis in plant cells. Nature **452:** 483–486

Outlaw WH, Manchester J (1979) Guard cell starch concentration quantitatively related to stomatal aperture. Plant Physiol **64:** 79–82

Perales M, Eubel H, Heinemeyer J, Colaneri A, Zabaleta E, Braun HP (2005) Disruption of a nuclear gene encoding a mitochondrial gamma carbonic anhydrase reduces complex I and supercomplex I + III2 levels and alters mitochondrial physiology in *Arabidopsis*. J Mol Biol **350:** 263–277

Raven JA (2001) An aquatic perspective on the concepts of Ingestad relating plant nutrition to plant growth. Physiol Plant **113:** 301–307

So AK, Espie GS, Williams EB, Shively JM, Heinhorst S, Cannon GC (2004) A novel evolutionary lineage of carbonic anhydrase (epsilon class) is a component of the carboxysome shell. J Bacteriol **186:** 623–630

Somersalo E, Occhipinti R, Boron WF, Calvetti D (2012) A reaction-diffusion model of CO_2 influx into an oocyte. J Theor Biol **309:** 185–203

Spalding MH (2008) Microalgal carbon-dioxide-concentrating mechanisms: chlamydomonas inorganic carbon transporters. J Exp Bot **59:** 1463–1473

Studer AJ, Gandin A, Kolbe AR, Wang L, Cousins AB, Brutnell TP (2014) A limited role for carbonic anhydrase in C_4 photosynthesis as revealed by a *ca1ca2* double mutant in maize. Plant Physiol **165:** 608–617

Tian W, Hou C, Ren Z, Pan Y, Jia J, Zhang H, Bai F, Zhang P, Zhu H, He Y, et al (2015) A molecular pathway for CO_2 response in Arabidopsis guard cells. Nat Commun **6:** 6057

Tripp BC, Smith K, Ferry JG (2001) Carbonic anhydrase: new insights for an ancient enzyme. J Biol Chem **276:** 48615–48618

Vahisalu T, Kollist H, Wang YF, Nishimura N, Chan WY, Valerio G, Lamminmäki A, Brosché M, Moldau H, Desikan R, et al (2008) SLAC1 is required for plant guard cell S-type anion channel function in stomatal signalling. Nature **452:** 487–491

Villarreal F, Martín V, Colaneri A, González-Schain N, Perales M, Martín M, Lombardo C, Braun HP, Bartoli C, Zabaleta E (2009) Ectopic expression of mitochondrial gamma *carbonic anhydrase 2* causes male sterility by anther indehiscence. Plant Mol Biol **70:** 471–485

von Caemmerer S, Lawson T, Oxborough K, Baker NR, Andrews TJ, Raines CA (2004) Stomatal conductance does not correlate with photosynthetic capacity in transgenic tobacco with reduced amounts of Rubisco. J Exp Bot **55:** 1157–1166

Wang Y, Duanmu D, Spalding MH (2011) Carbon dioxide concentrating mechanism in *Chlamydomonas reinhardtii*: inorganic carbon transport and CO_2 recapture. Photosynth Res **109:** 115–122

Witte CP, Noël LD, Gielbert J, Parker JE, Romeis T (2004) Rapid one-step protein purification from plant material using the eight-amino acid StrepII epitope. Plant Mol Biol **55:** 135–147

Xue S, Hu H, Ries A, Merilo E, Kollist H, Schroeder JI (2011) Central functions of bicarbonate in S-type anion channel activation and OST1 protein kinase in CO_2 signal transduction in guard cell. EMBO J **30:** 1645–1658

Yang Y, Costa A, Leonhardt N, Siegel RS, Schroeder JI (2008) Isolation of a strong *Arabidopsis* guard cell promoter and its potential as a research tool. Plant Methods **4:** 6

Young JJ, Mehta S, Israelsson M, Godoski J, Grill E, Schroeder JI (2006) $CO(_2)$ signaling in guard cells: calcium sensitivity response modulation, a $Ca(^{2+})$-independent phase, and $CO(_2)$ insensitivity of the *gca2* mutant. Proc Natl Acad Sci USA **103:** 7506–7511